Influence of electron-phonon interaction on the optical properties of III nitride semiconductors

2001 J. Phys.: Condens. Matter 13 7053

(http://iopscience.iop.org/0953-8984/13/32/312)

INSTITUTE OF PHYSICS PUBLISHING JOURNAL OF PHYSICS: CONDENSED MATTER

J. Phys.: Condens. Matter **13** (2001) 7053–7074 PII: S0953-8984(01)24815-2

Influence of electron–phonon interaction on the optical properties of III nitride semiconductors

X B Zhang, T Taliercio, S Kolliakos and P Lefebvre

Groupe d'Etude des Semiconducteurs, CNRS, Université Montpellier II, Case courrier 074, F-34095 Montpellier Cedex 5, France

Received 14 May 2001
Published 26 July 2001
Online at stacks.iop.org/JPhysCM/13/7053

Abstract

The electronic band structures of III nitride semiconductors calculated within the adiabatic approximation give essential information about the optical properties of materials. However, atoms of the lattice are not at rest; their displacement away from the equilibrium positions perturbs the periodic potential acting on the electrons in the crystal, leading to an electron–phonon interaction energy. Due to different ways that the lattice vibration perturbs the motions of electrons, there are various types of interaction, such as Fröhlich interaction with longitudinal optical phonons, deformation-potential interactions with optical and acoustic phonons and piezoelectric interaction with acoustic phonons. These interactions, especially the Fröhlich interaction, which is very strong due to the ionic nature of III nitrides, have a great influence on the optical properties of the III nitride semiconductors. As a result of electron–phonon interaction, several phenomena, such as phonon replicas in the emission spectra, homogeneous broadening of the excitonic line width and the relaxation of hot carriers to the fundamental band edge, which have been observed in GaN and its low dimensional heterostructures, are reviewed.

1. Introduction

GaN and its low dimensional structures have been extensively investigated in the past years due to their excellent optical and electrical properties. Progress in this field is so fast that the nitrides are expected to revolutionize the optoelectronics and electronics in the new century. The nature of high thermal conductivity, high luminous efficiency and mechanical robustness have made GaN and its alloys the superior material system for light emitting devices operated from the UV to the entire visible spectra region [1]. In addition, new applications in high power, high temperature and high frequency electronic devices based on GaN field effect transistors and heterobipolar transistors is under extensive exploration.

Despite their viable technological applications and remarkable achievements, the fundamental intrinsic properties, such as electron–phonon interaction, and physical parameters

of the III nitride materials, are less understood. While those extrinsic effects such as growth generated defects, fabrication induced defects, which degrade the device operation, can be controlled through the improved methods of growth and fabrications, the intrinsic properties cannot be controlled but must be understood since they play an essential role in the device operations. The intrinsic properties are mainly governed by the motion of the valence electrons in the crystal, which is a many body effect. There is no realistic way to solve the Hamiltonian involving a large number of electrons and nuclei. Approximations have to be introduced, such as the well known adiabatic approximation, in which the electrons are assumed to instantaneously follow the motions of the ion core of the lattice atom. This approximation is based on the fact that the ion core of the lattice atom is three to five orders of magnitude heavier than the electron. In the context of this approximation, the Hamiltonian for the total crystal system can be expressed as the sum of an electronic part H_e, of a lattice vibrational part H_{ph} and of an electron–lattice interaction part H_{e-ph}. The electronic and lattice vibrational parts can be treated individually, while the electron–lattice interaction is treated as a perturbation.

In the past years, various methods have been developed in order to calculate the electronic band structure of wurzite III nitride semiconductors [2–4]. Generally, for III–V nitride semiconductors with a wurtzite structure belonging to the space group C_{6v}^4, the conduction band minimum locates at the centre of Brillouin zone and its vicinity is almost entirely composed by the s states of nitrogen and cation atoms. The valence band maximum also locates at the centre of Brillouin zone and its vicinity is almost entirely composed by the p states of nitrogen. Due to the reduced symmetry and to the spin–orbit interaction, the valence band splits into the well known A, B and C bands with Γ_9, Γ_7, and Γ_7 symmetry, respectively. The conduction band has the Γ_7 symmetry. The valence band dispersion relations are anisotropic and strongly $\boldsymbol{k}$ dependent.

When solving the lattice vibrational part of the Hamiltonian, various methods have been used to calculate the phonon dispersion curves [5–13]. A group theory analysis of phonons at the Γ point of the Brillouin zone predicts the following set of eight modes: $(2A_1 + 2B_1 + 2E_1 + 2E_2)$, which belong to the irreducible representations of the C_{6v}^4 space group. Among them, the acoustic modes Γ_{ac} have $A_1 + E_1$ symmetries; the optical modes Γ_{opt} have $A_1+2B_1+E_1+2E_2$ symmetries. The A_1 and E_1 optical modes are both Raman and infrared active, the E_2 modes are only Raman active and the B_1 modes are silent. The frequencies and the properties of the six optical modes, $A_1(TO) + A_1(LO) + E_1(TO) + E_1(LO) + 2E_2$, have been widely investigated by the first-order Raman scattering [5, 12–16]. The phonons in AlGaN and GaInN alloys were also calculated and investigated by Raman spectroscopy. This showed that the phonons in GaInN alloys display a one-mode behaviour, while that in AlGaN alloy is complicated: the LO phonon displays a one-mode behaviour, but both one-mode and two-mode behaviours have been reported for the TO phonon [17–20].

The influence of phonons on the motion of electrons is treated as a perturbation. Due to the different ways they perturb the motion of electrons, there are various types of electron–phonon interaction [21], such as Fröhlich interaction with longitudinal optical (LO) phonons, deformation-potential interaction with both optical and acoustic phonons and piezoelectric interaction with acoustic phonons. The Fröhlich interaction is a Coulomb interaction between electrons and the longitudinal electric field produced by the LO phonons. The deformation-potential interaction is caused by the displacement of atoms from equilibrium positions, which affects the electronic band structure similarly to the effect of applying a strain. In non-centrosymmetric crystals, the strain field produces the electric field through the piezoelectric effect. Acoustic phonons can be piezoelectric active in certain directions. The piezoelectric interaction of electrons with acoustic phonons is similar to the Fröhlich interaction with LO phonons. The interactions of electrons with phonons have been demonstrated to greatly affect

the optical and electrical properties of semiconductors. As a result of the interaction, phonons can participate both in the near-band emission and in the absorption processes, which leads to an enhanced absorption near the fundamental band edge and broadens the emission peak. The cooling of hot carriers is also governed by the electron–phonon interactions. For the electrical properties, the interaction with phonons will scatter the electron from one state to another state, which results in a reduction of carrier mobility and an increase in resistivity. The basic knowledge of electron–phonon interaction is very important for improving the device operations.

In this paper, we review the influence of lattice vibration on the optical properties of nitride semiconductors and present recent studies of the electron–phonon interaction in this system. Several phenomena such as phonon replicas in the emission spectrum, broadening of excitonic line width and the cooling of hot carriers in GaN and its low dimensional structures, are discussed.

2. Basic theory of electron–phonon interaction

In most cases, the electrons in the conduction bands and holes in the valance bands are created and annihilated in pairs; we can rewrite the electron–phonon interaction Hamiltonian in terms of exciton–phonon interaction H_{ex-ph} [22]:

$$H_{ex-ph} = \sum_{n,n',k,q} V^{nn'}(q) B^{+}_{n,k+q} B_{n',k}(a_q + a^{+}_{-q}) \tag{1}$$

where (B^+, B) and (a^+, a) are exciton and phonon operators, respectively. $V^{nn'}$ is the matrix element for exciton–phonon interaction. The exciton–phonon interaction is usually weak and can be written as the sum of electron–phonon and hole–phonon interactions acting separately on the electron and hole bound in the exciton complex. In this case, $V^{nn'}(q)$ can be written as [22, 23]:

$$V^{nn'}(q) = \int \mathrm{d}^3 r \phi^*_n(r)\phi_{n'}(r)[F^e_q \exp(-\mathrm{i}qrm_e/M) - F^h_q \exp(\mathrm{i}qrm_h/M)] \tag{2}$$

where m_e and m_h are the electron and hole masses, respectively. $M = M_e + m_h$ is the total mass. $\phi_n(r)$ is the exciton wave function for quantum number n. F^e_q and F^h_q are electron– and hole–phonon coupling constants, respectively.

For the interaction of the exciton with the acoustic phonon, two types of interaction have been considered. The first one is the deformation potential interaction, for which we have

$$F^{e(h)}_q = \sqrt{\frac{\hbar}{2\rho v V q}} D_{e(h)} \tag{3}$$

where ν is the velocity of sound, ρ the density of the crystal and D_e and D_h are the deformation potential constants of the conduction band and valence band, respectively. Since the transverse acoustic (TA) phonons produce a shear strain and hence have a smaller deformation potential than the longitudinal acoustic (LA) phonons, the dominant contribution is from the LA phonons. The second type is the piezoelectric interaction, which in wurtzite structures is written [24]

$$F^e_{q,TA(LA)} = F^h_{q,TA(LA)} = \frac{4\pi e}{\varepsilon_0}\sqrt{\frac{\hbar}{2\rho v_{TA(LA)} q}}[e_{15}\sin^2\theta(U_z\sin\theta + U_y\cos\theta) + e_{13}U_y\sin\theta\cos\theta + e_{33}U_z\cos^2\theta] \tag{4}$$

where v_{TA}, v_{LA} are the transverse and the longitudinal sound velocities, respectively. $U_i (i = x, y, z)$ is the displacement of atoms in the unit cell. θ is the angle between $\vec{q}$ and the z axis, and the e_{15}, e_{33}, e_{13} are the nonzero components of the piezoelectric tensor. The angular factors in the above equation can be spherically averaged to give effective piezoelectric constants for LA and TA phonons, respectively.

$$\langle e_{LA}^2 \rangle_\theta = \tfrac{1}{7} e_{33}^2 + \tfrac{4}{35} e_{33}(e_{31} + 2e_{15}) + \tfrac{8}{105}(e_{31} + 2e_{15})^2 \tag{5}$$

$$\langle e_{TA}^2 \rangle_\theta = \tfrac{2}{35}(e_{33} - e_{31} - e_{15})^2 + \tfrac{16}{105} e_{15}(e_{33} - e_{31} - e_{15}) + \tfrac{16}{35} e_{15}^2. \tag{6}$$

The interaction of the exciton with nonpolar transverse optical (TO) phonons can be simply described as a deformation potential. This mechanism of interaction can be written as [25]

$$F_q^{e(h)} = \sqrt{\frac{\hbar}{2\mu N \omega}} \frac{\Xi_{e(h)}}{a} \tag{7}$$

where μ is the reduced mass of the atoms in the unit cell, N is the number of unit cells in the crystal, a is the lattice constant and $\hbar\omega$ the optical phonon energy.

In the case of LO phonons, besides the nonpolar deformation potential interaction, there is an additional interaction due to the Coulomb interaction between the electric field and the charges in the exciton. It is known as the Fröhlich interaction. F_q for the Fröhlich interaction is

$$F_q^e = F_q^h = \left[\frac{2\pi e^2 \hbar \omega_{LO}}{V q^2} (\varepsilon_\infty^{-1} - \varepsilon_0^{-1}) \right]^{\frac{1}{2}} \tag{8}$$

where $\hbar\omega_{LO}$ is the LO phonon energy, V is the crystal volume and ε_∞, ε_0 are the high- and low-frequency dielectric constants. In wurtzite III nitride semiconductors, the A_1(TO) and E_1(TO) phonons are not purely transverse modes; the Fröhlich interaction with these TO-like modes can be strongly enhanced over a range of angles with respect to the c axis [26]. The Fröhlich interaction with the LO-like modes, i.e., A_1(LO) and E_1(LO), is similar to equation (8) [26]. Due to the strong ionic nature of the nitride semiconductors, the Fröhlich interaction is the strongest one among all interactions. It plays a dominant role in determining the cooling of hot carriers and the band edge optical transitions, which will be addressed in the sections below.

3. LO phonon replica

A most important result of the exciton–phonon interactions in semiconductors is the appearance of phonon-assisted emissions of free and bound excitons in the luminescence spectra. In the past decades, phonon replicas have been observed in the photoluminescence (PL) spectra in most II–VI semiconductors [27–31] and in some ionic crystals [32]. Their origin has been thoroughly investigated. The distribution of the emission intensities between the main peak and the phonon replicas has been found to depend strongly on the exciton–phonon coupling strength. Within the Franck–Condon approximation, this coupling is expressed by the Huang–Rhys factor S [33]. At low temperature, the relationship between the intensity of the nth phonon replica I_n and the main emission I_0 is given by

$$I_n = I_0 \frac{S^n}{n!} \qquad n = 0, 1, 2, \ldots \tag{9}$$

where the S factor is defined as [33–35]

$$S = \sum_q \frac{|V(q)|^2}{(\hbar\omega_{LO})^2} \tag{10}$$

$V(q) = \int \mathrm{d}^3 r \phi(r)^2 [F_q^e \exp(-\mathrm{i}qrm_e/M) - F_q^h \exp(\mathrm{i}qrm_h/M)]$. The parameters in $V(q)$ have been discussed in section 2. Since the LO phonon Fröhlich interaction is the strongest, usually only the LO phonon replicas are observed. Thus, usually, the Fröhlich interaction is taken into account in calculating $V(q)$. The S value for LO phonons therefore depends on the ionic nature of the semiconductor and on the separation of Fourier transformed charge distributions of electron and hole.

For bound excitons, S depends on the spreading of the wave function of the bound exciton in wave vector k-space. In the case of shallow donors or acceptors, the extension of the wave function in k-space is restricted to the vicinity of the Brillouin zone centre. Only those phonons with wave numbers close to the Brillouin zone centre can participate in the emission process. The Huang–Rhys factor S for a bound exciton can be written as [34, 36]

$$S = \frac{e^2}{\hbar\omega_{LO}} \left(\frac{1}{\varepsilon_\infty} - \frac{1}{\varepsilon_0} \right) \int |\rho(q)|^2 \mathrm{d}^3 q \tag{11}$$

where $\rho(q)$ is the Fourier transform of the charge density. In the limiting case of the hydrogen-like impurity, the S factor can be simplified as [34]

$$S = \frac{e^2}{\hbar\omega_{LO}} \left(\frac{1}{\varepsilon_\infty} - \frac{1}{\varepsilon_0} \right) \frac{5}{16a^*} \tag{12}$$

where a^* is the effective Bohr radius of the impurity.

For a free Wannier exciton in the lowest-lying 1S state, the maximum value of $V(q)$ is at $q \approx 1/a_B$ [31], where a_B is the Bohr radius of the 1S exciton. In this case, the S value for the free exciton is similar to those for hydrogen-like impurities and is proportional to $1/a_B$ [37]. The free exciton can migrate in the crystal and has a kinetic energy. Those excitons with centre of mass wave vector $K \neq 0$ are not allowed to recombine radiatively due to the momentum conservation law. The interaction with LO phonon transfers the momentum to the phonon, thus allowing the exciton to recombine radiatively. The sum in equation (10) is over those phonons which satisfy the momentum transfer. Detailed investigations of the line shape of LO phonon replicas showed that the shape of phonon replicas represents with a good accuracy the equilibrium Maxwell distribution of the exciton kinetic energies and can be expressed as the following power law equation [27, 28, 31]:

$$I_n(E) \propto E^{\frac{1}{2}} \exp(-E/kT) W_n(E) \tag{13}$$

where $E^{\frac{1}{2}}$ reflects the density of states in the parabolic exciton band (valid for a three-dimensional bulk crystal). The exponential term reflects the exciton statistics, which can be taken as a Maxwell–Boltzmann distribution at low excitation intensities. T is the lattice temperature. $W_n(E)$ is the probability that the free exciton of a given kinetic energy E recombines via the nth phonon assisted process. For the 1LO phonon assisted process, experimentally, it is found that the probability $W_1(E)$ is proportional to the exciton kinetic energy E. Based on a simple argument, when q is small, it is theoretically found that $W_1(E) \propto |V(q)|^2 \propto q^2$. Due to the conservation of momentum in the phonon assisted recombination process, $q \approx K$. Thus, $W_1(E)$ is also proportional to the exciton kinetic energy.

For the second LO phonon assisted processes, it is experimentally found that the probability $W_2(E)$ is independent of the exciton kinetic energy [28]. Theoretically, a perfect calculation of $W_2(E)$ should include the scattering of exciton from the 1S state through the intermediate states, involving discrete and continuum exciton states, to the final radiative state by emission of two LO phonons [27, 31]. It is impractical to calculate this sum of intermediate states exactly. After several simplifications [27], it was shown that the line shape of the second LO

phonon replica around the threshold is also independent of the exciton kinetic energy. The independence of the line shape of $I_2(E)$ of the exciton kinetic energy has an experimental importance. It gives direct information about the concentration and about the distribution of free excitons in the semiconductor.

The above power law line shape of the LO phonon replicas results in the following important predictions [31]:

(1) the line shape of the phonon replica is asymmetric. Its peak energy depends on the temperature. The shift Δ of the line maximum from its low energy threshold increases linearly with temperature, i.e., $\Delta = \frac{3}{2}kT$ for the 1LO and $\Delta = \frac{1}{2}kT$ for the 2LO phonon replica;
(2) the line width also increases linearly with temperature: the line width is $3kT$ for the 1LO and $2kT$ for the 2LO replica;
(3) the ratio of the integrated intensity of the 1LO replica to that of the 2LO replica, i.e., I_{1LO}/I_{2LO}, also depends linearly on temperature.

These predictions show that the lattice temperature has a great influence on the distribution of luminescence among the LO phonon replicas and the zero phonon line.

The LO phonon replicas of free and bound excitons in GaN were observed 30 years ago [38], but it was only recently, with the breakthrough in the growth methods and the improvement in the quality of GaN material, that the LO phonon replicas in GaN could be systematically studied. The study of the LO phonon replica in GaN showed that the physics of the phonon replica, obtained mostly in II–VI semiconductors, works well when applied to nitride semiconductors [39–43, 45–48]. Figure 1 shows a typical temperature dependent PL study of an undoped GaN sample [39, 40]. At low temperatures, the spectra are dominated by neutral donor bound exciton emission (I_2 line). Free exciton A and B emissions are also seen in the spectra. At the low energy side of these main peaks, two groups of peaks can be well resolved in the spectra. The peaks marked as A–LO (I_2–LO) and A–2LO (I_2–2LO) correspond to the recombinations of an A exciton (neutral donor bound exciton) with emission of 1LO and 2LO phonons, respectively. The emission band near 3.27 eV comes from the donon–acceptor pair (DAP) recombinations; their 1LO phonon replica around 3.18 eV is also seen in the spectra. A close investigation of the spectrum at 9 K shows that the Huang–Rhys factor S for the free exciton A, neutral donor bound exciton I_2 and DAP recombinations are around 0.0077, 0.0013 and 0.7, respectively. The values of S factor for the free exciton and for the neutral donor bound exciton are close to those reported in [47]. The small value of S for the neutral donor bound exciton indicates that the coupling between the LO phonon and the neutral donor bound exciton is weak. This weak coupling is caused by the smaller spreading of the wave function of the donor bound exciton in k-space. Thus fewer phonons are involved in the coupling [41]. The large S value for DAP is due to the fact that the S value of DAP depends on both the distance between and the localization of charges at the donor and the acceptor centres [34, 36]. The more distant the donor and acceptor pair, the larger the S value observed. A slightly smaller S value of 0.6 for DAP was also reported in GaN [43]. This is possibly due to the difference in excitation intensity in these PL measurements. Since the value of S for DAP is very sensitive to the distance between the donor and acceptor pair, increasing the excitation intensity would make the closer DAP have more chance to recombine. Thus, a smaller value of S is expected [44].

With an increase in temperature, the I_2 line progressively quenches to the benefit of the free exciton line A. The free exciton line A becomes the dominant one in the spectrum at temperature of 100 K. Relative to the free exciton A, the intensity of the A–1LO replica becomes remarkable at higher temperatures. This indicates that the coupling strength between the free exciton A and

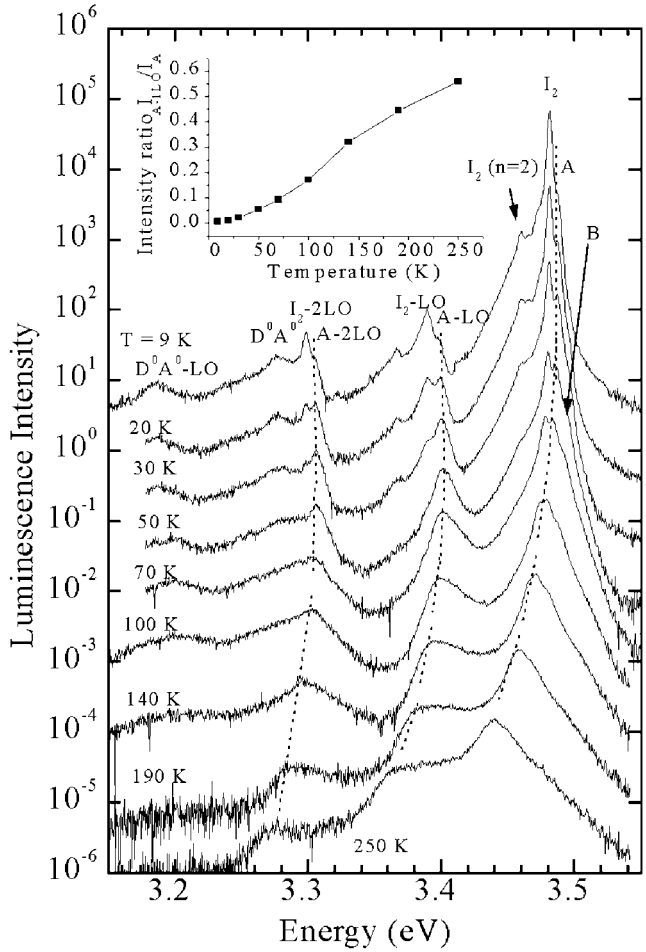

Figure 1. Temperature dependent PL spectra of a high quality undoped GaN sample. The temperature for each spectrum is indicated in the figure. The inset of the figure shows the intensity ratio of I_{A-1LO}/I_A as a function of temperature (after [40]).

the LO phonon increases with an increase in temperature. This increase in coupling strength is clearly shown in the inset of the figure and has been observed by other groups [43, 47]. Within Segall and Mahan's theory [27], the phonon assisted excitonic transition probability depends on the kinetic energy of the exciton (equation (13)). Since the kinetic energy of the exciton increases with the temperature, an increase in intensity ratio I_{nLO}/I_0 with the temperature would be expected. Various values of S factor reported by different authors might be due to the temperature effect [45–48]. With an increase in temperature, the linewidths of A–LO replicas become broader. The influences of temperature on the intensity and the linewidth of A–LO replicas agree very well with the theoretical predictions [31]. The dotted lines in the figure indicate the temperature variation of the peak energy of A exciton and its phonon replicas. The peak energy of the A exciton tracks the bandgap of bulk GaN in the whole temperature range, while for the 1LO and 2LO phonon replicas, the temperature shifts of the peak energies are small. The smaller shifts also agree well with the theoretical predictions as shown above. The line shape of phonon replicas shows some departure from equation (13),

possibly due to the scattering by point defects [49]. The temperature dependent line shape and line width of LO phonon replicas, and the temperature dependent intensity ratio of the 1LO to 2LO replica in a high quality GaN sample agree well with the three predictions [45–47].

Nitride semiconductors are known for their high efficiency in luminescence despite the huge densities of defects. Study of the defect properties may give additional knowledge on the device performance. It has been found that defects not only affect the distribution of luminescence between the zero phonon peak and the phonon replicas, but also modify the shape of the LO phonon replicas [49]. When GaN contains a high density of residual donors, the efficiency of phonon assisted free excitonic recombination is low and a deviation of the line shape of the 1LO phonon replica from equation (13) is observed [49]. It was speculated that the unusual observations were caused by the enhanced scattering of the exciton–polariton into the radiative branch of the zero phonon free exciton A by point or extended defects, which assist the momentum transfer. In another report [50], a similarly low efficiency of phonon assisted free excitonic recombination was observed in GaN with p-type doping. The origin was also considered to be the defect enhancement of the scattering [50]. Later in a PL study of GaN films grown with different polarity, it was found that the polarity of the GaN film also has a great influence on the observation of LO phonon replicas [51]. When growing samples on a Ga-terminated surface, relative to the zero phonon peak, the LO phonon replicas are strong, whereas when growing on an N-terminated surface, the replica is hardly seen. Since the polarity affects the growth mode and thus affects the incorporation of defects in GaN epilayers, the incorporated defects were also thought to rule the observation of phonon replicas. Recently, the influence of crystal polarity on the observation of phonon replicas in the PL spectrum was studied in ZnO film [52], where the phonon replicas are much stronger in the PL spectra measured from the O-terminated surface than from Zn-terminated surface. Note that the effect of polarity is reversed in ZnO. However, it is argued that the Zn surface is easier to contaminate. A defect mechanism was also thought to be responsible for the observations.

4. Band edge excitonic linewidth

The band edge optical properties of GaN are dominated by excitonic effects even at room temperature. Such excitonic effects strongly affect the linear and nonlinear optical properties of the material and hence have interest in device applications. The interactions between excitons and phonons, however, will ionize the exciton into a free electron and hole in the continuum of states or scatter the exciton into discrete exciton states. At low temperatures, since the population of the LO phonon is vanishingly small, the scattering is mainly ruled by acoustic phonons. At high temperatures, the LO phonon Fröhlich scattering dominates. The lifetime of exciton, as a result of the scattering by phonons, will be significantly reduced at high temperatures. An increase in homogeneous linewidth of the exciton can be observed in the temperature dependent absorption or emission or reflectance spectra. Conversely, study of the temperature dependent excitonic linewidth will provide important information about the exciton–phonon interactions.

According to Segall's expression [22], the total linewidth of the exciton contains two contributions: inhomogeneous broadening and homogeneous broadening. Within the adiabatic approximation, the linewidth of the lowest-lying 1S exciton state can be written as

$$\Gamma(T) = \Gamma_0 + \gamma_{ph} T + \Gamma_{LO} N_{LO} \tag{14}$$

where Γ_0 is the inhomogeneous linewidth due to the exciton–exciton, exciton–carrier interaction [53], and the scattering by defects, impurities and alloy fluctuations. In low dimensional heterostructures, the size fluctuations also contribute to Γ_0. It is independent of

temperature. The second term $\gamma_{ph}T$ is due to the acoustic phonon scattering. The γ_{ph} represents the acoustic phonon coupling strength, mainly caused by the deformation potential mechanism. The T in $\gamma_{ph}T$ is a result of linear dependence of the acoustic phonon occupation number on the temperature T. In most semiconductors, due to the small sound velocity, the scattering by the acoustic phonon is within the same excitonic band state [22]. The third term is the linewidth due to the LO phonon scattering. Γ_{LO} is the exciton–LO phonon coupling strength, and $N_{LO} = 1/[\exp(\hbar\omega_{LO}/kT) - 1]$, is the LO phonon occupation number. For those excitons which are not in the lowest-lying states, the phonon occupation number N_{LO} is replaced with $2N_{LO} + 1$ [54], since both phonon absorption and emission processes can take place now.

Various models, slightly different from equation (14), appear in the literature. For example, a Bose–Einstein type expression, in which both acoustic and optical phonons are taken into account as an average effect on the excitonic linewidth, is used to describe the temperature dependent excitonic linewidth. The linewidth is written as [54]

$$\Gamma = \Gamma_0 + \Gamma_{ep}/[\exp(\theta/T) - 1] \tag{15}$$

where θ is an average of phonon temperature, Γ_{ep} is an exciton–average phonon coupling strength. This model gives information about the average strength of the exciton–phonon scattering by all phonon branches. In another model [55], scattering by ionized impurities is included in fitting the experimental linewidth. Care should be taken when using this model since more parameters are involved in the fitting process [56].

Temperature dependent linewidths of excitons in GaN have been measured by a variety of spectroscopic methods. These methods include absorption [57], PL [47, 58, 59], reflectance [60, 61], electroreflectance [62], spectroscopic ellipsometry [63] and femtosecond four-wave-mixing studies [64]. However, the mechanism responsible for the linewidth broadening is under debate. Scattering of excitons by different phonon branches and different models have been considered by different authors. In [57, 58, 60, 61, 64], both acoustic phonon and LO phonon scattering are considered, while in [59] and [61], instead of acoustic phonons, the authors showed that scattering by the low frequency branch of the E_2 phonon gives a better fit to the experiment linewidth. In [62, 63], the contribution by the acoustic phonon is completely neglected; an exciton–average LO phonon interaction model was used to fit the experimental results. In [47], a complicated model, involving contributions of the acoustic phonon and the average LO phonons, was used to fit the experimental linewidth. Table 1 summarizes the exciton–phonon coupling parameters, obtained by fitting the experimental linewidth, and measured by various spectroscopic methods in these reports.

The parameter Δ in the table is a homogeneous linewidth at 300 K, calculated by the model used in the reference. From the table, it is clearly seen that the values for exciton–phonon coupling strength, even obtained by considering the same model, are not consistent. The values cover a wide range. We note that the calculated Δ, which represents the observed homogeneous linewidth at 300 K very well, is much smaller when the spectra were measured by reflectance spectroscopic technique, and is much larger by PL. The other methods give the moderate values of Δ. This difference suggests that the mechanism for linewidth broadening or errors generated during the fitting of the experimental results is different from measurement to measurement. The excitonic linewidths deduced from the reflectance spectra are indirectly related to the near band edge density of states. In [58, 62], the inhomogeneous linewidths of free excitons A and B are larger than the homogeneous ones at 300 K. Moreover, the A and B excitons are not well resolved even at very low temperature. This may plague the analysis of experimental linewidth [58, 62], and errors would be generated during the fitting of the experimental results. In PL measurements, when at high temperatures, the linewidths of A and B excitons are much broader than the separation between the A and B peaks [65], the two

Table 1. Reported linewidth parameters for free exciton transitions in GaN.

Method	Γ_0 (meV)	γ_{ph} (μeV K^{-1})	Γ_{LO} (meV)	Γ_{ep} (meV)	θ (K)	Γ_{EI} (meV)	Δ (meV)
[a] Absorption (A exciton)	10	15	375				15.6
[b] PL (A exciton)	2.8	21	525				21.9
[b] PL (B exciton)	1.4	22	495				21.3
[c] PL (A exciton)	5.69		165			10	15.0
[d] PL (A exciton)	3.15	41.8		140	748		25.2
[e] Reflectance (A exciton)	∼1.5	15.3	208				10.8
[f] Reflectance (A exciton)	2.4	9.5	295				11.6
[f] Reflectance (A exciton)	2.4		220			3.7	10.3
[g] Electroreflectance (A exciton)	15			60	731		5.7
[g] Electroreflectance (B exciton)	13			74	773		6.1
[h] Spectroscopy ellipsometry	34			104	800		7.8
[i] Four-wave-mixing (A exciton)	2.4	16	390				16.4
[i] Four-wave-mixing (B exciton)	2.5	13	470				17.8

[a] Fischer A J, Shan W, Song J J, Chang Y C, Horning R and Goldenberg B 1997 *Appl. Phys. Lett.* **71** 1981
[b] Viswanath A K, Lee J I, Kim D, Lee C R and Leem J Y 1998 *Phys. Rev.* B **58** 16 333
[c] Chichibu S, Okumura H, Nakamura S, Feuillet G, Azuiiata T, Sota T and Yoshida S 1997 *Japan. J. Appl. Phys.* **36** 1976
[d] Liu W, Li M F, Xu S J, Uchida K and Matsumoto K 1998 *Semicond. Sci. Technol.* **13** 769
[e] Korona K P, Wysmolek A, Pakula K, Stepniewski R, Baranowski J M, Grzegory I, Lucznik B, Wroblewski M and Porowski S 1996 *Appl. Phys. Lett.* **69** 788
[f] Siozade L, Colard S, Mihailovic M, Leymarie J, Vasson A, Grandjean N, Leroux M and Massies J 1999 *Phys. Status Solidi* b **216** 73
[g] Li C F, Huang Y S, Malikova L and Pollak F H 1997 *Phys. Rev.* B **55** 9251
[h] Petalas J, Logothetidis S, Boultadakis S, Alouani M and Wills J M 1995 *Phys. Rev.* B **52** 8082
[i] Fischer A J, Shan W, Park G H, Song J J, Kim D S, Yee D S, Horning R and Goldenberg B 1997 *Phys. Rev.* B **56** 1077

transitions will overlap significantly. This overlap, together with an increase in the relative intensity of the B exciton at high temperature, would also make the experimental results difficult to fit. Errors would be generated during the fitting. It has been argued that four-wave-mixing studies might give the most accurate parameters presently for exciton–phonon coupling strength, since the excitonic features are several orders of magnitude stronger and the background, coming from the contribution of free carriers, is significantly suppressed [58, 64]. Improving the quality of GaN may give more accurate values of exciton–phonon coupling strengths in the measurements.

It is interesting to compare Γ_{LO} in GaN with those in other III–V semiconductors and II–VI semiconductors. The Γ_{LO} values for GaAs [66], ZnSe [67], CdTe [22], CdS [22] and ZnO [68] are 5, 81, 17, 41 and 876 meV, respectively. It can be seen that the values of Γ_{LO} in GaN, obtained by various methods, are much larger than those in GaAs and in most II–VI semiconductors. The large value of Γ_{LO} suggests that the exciton–LO phonon Fröhlich interaction significantly affects the room temperature and high temperature performances of GaN-based devices.

5. Cooling of hot carriers in GaN

Nitride semiconductors are known for their applications in high power and high temperature devices. Therefore knowledge about the fundamental relaxation process of hot carriers and their distributions is very important for device engineers. Optical excitation of semiconductors at energies well above the band gap is followed by a rapid relaxation in both momentum and energy of the photo-generated carriers. A variety of scattering processes contribute to the relaxation of hot electrons and holes and affect their distributions. There may be electron–electron scattering, hole–hole scattering, electron–hole scattering, electron–phonon interactions, hole–phonon interactions and phonon–phonon interactions. Their relative importance in the relaxation of hot carriers is determined by the actual experimental conditions, in particular by the photon energy and the intensity of exciting laser light, and by the lattice temperature. Carrier–carrier scattering leads to the relaxation of both momentum and energy in the carrier system and drives the monochromatic or quasi-monochromatic energy distribution of carriers into a quasi-equilibrium distribution. The scattering rate depends strongly on the carrier density [69, 70]. Interactions with phonons transfer the excess energy of the carrier system to the lattice by creation of various phonons. The phonon–phonon interaction will affect the efficiency of this energy transfer.

The excitation intensity, and thus the density of carriers, has a great influence on the carrier–carrier scattering rates [71]. With an increase in excitation intensity, the carrier–carrier scattering rate increases. A simple model predicts that the carrier–carrier scattering rate increases linearly with the carrier density [70]. There is a critical carrier density, below which the carrier–LO phonon interaction dominates, and above which the carrier–carrier scattering dominates. This critical density is about 10^{19} cm^{-3} in GaN [72]. In the following, we discuss the relaxation of hot carriers in the low and high excitation intensity regions.

At low excitation intensities, carrier–LO phonon interaction dominates. The carrier system loses its kinetic energy through a cascade emission of LO phonons before it is thermalized with a well defined temperature. In GaAs, the photo-excited electrons and holes are relaxed individually toward their respective band extrema by successive emission of LO phonons, until they do not have sufficient energy to emit a further LO phonon. The cooling of the remaining energy is followed by the acoustic phonon deformation potential interaction. In GaN, however, due to the large exciton binding energy, photo-generated electrons and holes directly form excitons assisted by emission of an LO phonon. The subsequent relaxation of the hot exciton occurs via a cascade emission of LO phonons. Evidence of this relaxation of electron–hole pairs comes from the PL excitation studies [46, 73]. The PL excitation spectra show periodic structure with an energy separation exactly equal to $\hbar\omega_{LO}$. Increasing the carrier density reduces the oscillation strength of the periodic structure.

At high excitation intensities, carrier–carrier scattering becomes more important. Moreover, the strengths of carrier–phonon interactions are greatly influenced by the high density of carriers [71]. The strength of carrier–phonon interactions is controlled by the hot phonon effect and the screening effect [71]. In GaN, the relative magnitudes of the energy loss rates, through the interactions with different branch of phonons, have been calculated in [74]. Figure 2 shows the energy loss rates of electrons and holes, through the polar LO phonon Fröhlich interaction, TO, LA phonon deformation potential interactions and the LA phonon piezoelectric interaction. In the case of electron–phonon interactions (figure 2(a)), the polar LO phonon interaction is the dominant one. At low carrier densities, it is about two orders of magnitude stronger than that of TO phonon deformation potential interaction, and four orders of magnitude stronger than the LA phonon piezoelectric interaction. Compared with the energy loss rates of electrons, a slight difference for holes can be seen in figure 2(b). The nonpolar

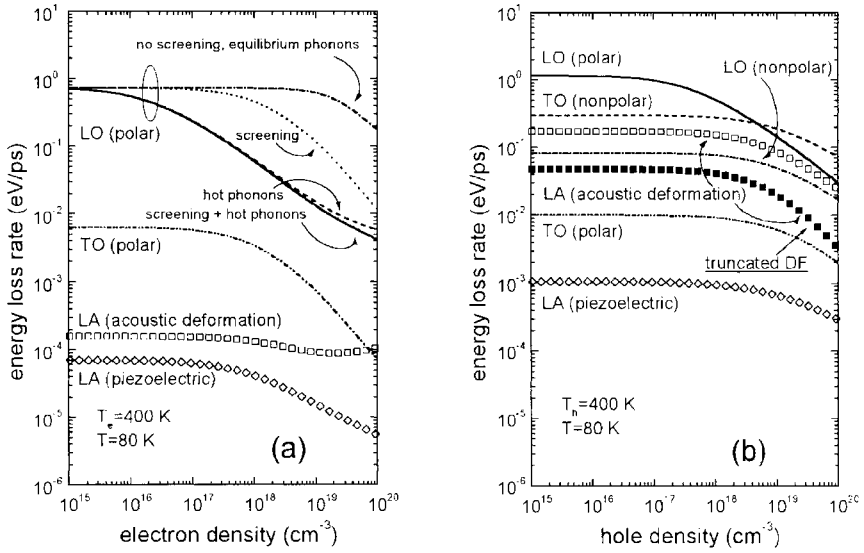

Figure 2. The energy loss rates of electrons (a) and holes (b), as a function of the carrier density. The energy loss rates due to the scattering by various phonon modes are indicated in the figure (after [74]).

interaction with TO phonon becomes as important as the polar interaction with LO phonons in relaxing the energy of holes, especially when the carrier density is high. Both interactions with LA phonon through deformation potential and piezoelectric mechanisms are greatly enhanced for holes. The energy loss rate, through the piezoelectric interactions with the TA phonons, which is not shown in figure 2, should be comparable to that through the interaction with the LA phonons [75]. A characteristic feature in the figure is that, at high carrier densities, due to the screening effect and hot phonon effect, the energy loss rate through the LO phonon emission reduces significantly, especially for electrons. A comparison between the screening and hot phonon effects shows that the hot phonon effect is the dominant one in reducing the energy loss rate. The hot phonons, generated by the relaxation of hot carriers, enable the hot carriers to have an increased probability of reabsorbing phonons. Thus, a reduction in energy loss rate of hot carriers is expected.

The lifetimes of phonons determine the hot phonon effect. At high excitation intensities, phonons, especially the LO phonons, which are created by the relaxation of hot carriers, do not have enough time to decay. A build-up of nonequilibrium phonon populations is expected. This phenomenon is evidenced from a low temperature Raman study [76]. Figure 3 shows the polarized Raman spectra of the GaN sample taken at 25 K. The sharp peak at 757 cm^{-1} in (a) is the scattering by E_g phonon of the substrate sapphire: the shoulder around 741 cm^{-1} comes from the A_1(LO) phonon of GaN. The peaks at 574 cm^{-1} and 538 cm^{-1} in spectrum (b) correspond to E_2 and A_1(TO) phonons, respectively. The anti-Stokes Raman spectra in (c) and (d) show that the A_1(LO) phonon is clearly seen but E_2 and A_1(TO) phonons are not. Similar results for E_1(LO) and E_1(TO) phonons in GaN are also observed. Under thermal equilibrium conditions, the ratio of anti-Stokes to Stokes intensities for a phonon mode in Raman spectra is proportional to $N_{LO}/(N_{LO}+1)$. For the LO phonon with $\hbar\omega_{LO} \sim 92$ meV, the ratio is below 10^{-10} at 25 K. Thus, the anti-Stokes peaks should be too weak to be observable at this temperature. The observation of anti-Stokes A_1(LO) and E_1(LO) peaks indicates that significant nonequilibrium LO phonons have been created in the material. The nonequilibrium

LO phonons are created by the relaxation of energetic electron–hole pairs, excited by incident laser light, through the strong Fröhlich interaction.

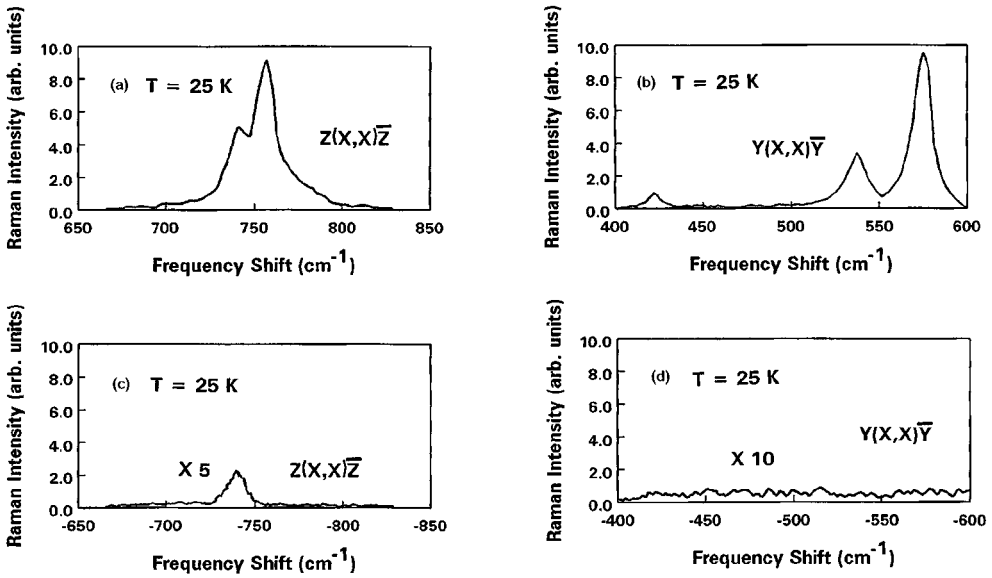

Figure 3. Polarized Stokes Raman spectra (a) and (b) and anti-Stokes Raman spectra (c) and (d). The spectra were measured from an undoped GaN sample at 25 K. The scattering geometry for each spectrum is indicated in the figure. Notice that the anti-Stokes Raman spectrum is multiplied by a factor of five in (c) and ten in (d) (after [76]).

In GaN, the lifetime of $A_1(LO)$ phonons, obtained from time resolved Raman study, is about 5 ps [77, 78], while in AlN, the lifetime of $A_1(LO)$ phonons, obtained from the phonon linewidth in Raman spectra, has been reported in a range from 0.45 to 0.75 ps [79, 80]. The lifetimes of phonons are determined by the anharmonic decay of a phonon into other low energy Brillouin zone phonons such that the energy and momentum are conserved [81, 82]. Crystal imperfections such as impurities and defects are also shown to affect the lifetimes of phonons, since the crystal imperfections can destroy the phonon propagation [80].

Besides the theoretical calculations, the rates of carrier–LO phonon interactions are also determined experimentally. The femtosecond pump and probe technique has been used to probe the relaxation rate of hot electrons in n-type doped GaN [83] and the relaxation rate of hot holes in p-type doped GaN [84]. In these reports, the measured LO phonon emission time is $\tau_e \sim 0.2$ ps for electrons and $\tau_h \sim 0.6$ ps for holes. These values are about 20 times larger than those calculated theoretically, possibly due to the hot phonon effect. The time for electron–LO phonon scattering, determined from subpicosecond time resolved Raman scattering, is $\sim$0.05 ps [85]. The scattering time for $E_1(LO)$ phonons is also around 0.05 ps. Considering the interaction with the two branches of LO phonons, it shows that the electron–LO phonon scattering rate in GaN is about one order of magnitude larger than that obtained in GaAs [85].

The hot phonons have a great influence on the exciton stability. When the occupation number of hot phonons is large, due to the scattering with hot phonons, excitons will be ionized even at very low temperature. As a result, electron and hole pairs lose their correlation immediately after their generation and rapidly form hot plasma, and are thermalized among themselves with a characteristic temperature much higher than the lattice temperature. This is known as the heating effect. The heating of the electron and hole plasma has a great influence

on the performance of GaN-related devices, which operate in the high injection regime. This heating effect is directly reflected by an enhancement of the high energy wing of the near band emission in PL spectra under high photo-excitations. Figure 4 shows the near band PL spectra of a GaN sample at a temperature of 80 K [86]. The excitation photon energy is 4.66 eV, thus the excess energy of a photo-created electron–hole pair is 1.18 eV, much larger than the energy of an LO phonon. Relaxation of hot carriers through a cascade emission of LO phonons is possible. At high excitation intensities, the hot phonon effect, which reduces the energy loss rate of the hot carriers, would be expected. If the characteristic temperature of the thermalized carriers has not reached the lattice temperature before the recombination takes place, the temperature of carriers will be reflected in the PL spectra. In this case, the high energy tail of the band edge PL can be well fitted by

$$I(\hbar\omega) \propto \exp[-(\hbar\omega - E_g)/kT_e] \tag{16}$$

where T_e is the carrier temperature. The fitted value of T_e for each spectrum, taken under different excitation intensity, is indicated in the figure. An increase in T_e with an increase in excitation intensity is clearly seen. A detailed analysis of the relationship between T_e and the excitation intensity suggests that hot holes are unable to establish a smooth distribution above the threshold of optical phonon emission before they recombine with electrons [86].

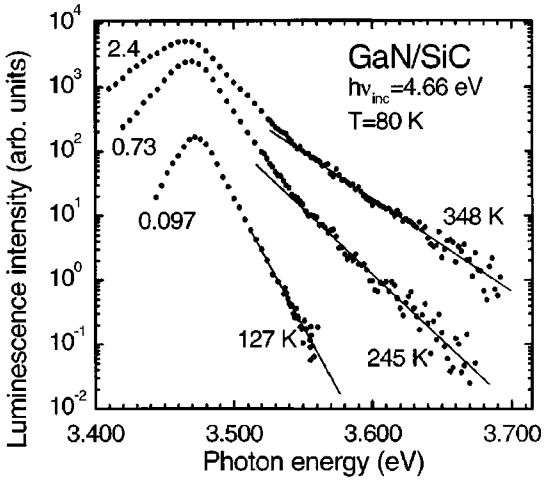

Figure 4. PL spectra of a GaN epilayer grown on SiC with a lattice background doping less than 10^{16} cm^{-3}. The exciting photon energy is 4.66 eV and the temperature is 80 K. The excitation power density in MW cm^{-2} for each spectrum is indicated on the left-hand side of the curve. The electron temperature is indicated on the right-hand side of the curves (after [86]).

The dynamic evolution of exciton temperature can be observed in the time resolved PL studies. In the case of low excitation conditions, the near band emission is dominated by excitonic transitions. A photo-excited hot exciton relaxes down by a cascade emission of LO phonons until its kinetic energy is not sufficient to emit an LO phonon further. The residual energy is dissipated primarily through the acoustic phonon interactions. Since the interaction with acoustic phonons is about three to four orders of magnitude weaker than that with LO phonons, the interaction of excitons among themselves will establish a quasi-equilibrium distribution with a characteristic temperature. However, the temperature of excitons cannot be extracted directly from the free exciton recombination line, since those excitons with momentum $K \neq 0$ are not allowed to recombine as a result of the momentum

conservation law. As discussed in section 3, the momentum selection rule can be relaxed by the participation of phonons in the recombination. The line shape of LO phonon replicas represents the Maxwell distribution of exciton kinetic energies with a characteristic temperature. The dynamic evolution of the shape of the LO phonon replica thus directly reflects the cooling process of excitons through the emission of acoustic phonons. By fitting the 1LO phonon replica of the free exciton in GaN with equation (13), the exciton temperature at each time, delayed after the excitation pulse, can be obtained. Figures 5(a) and (b) show the exciton temperatures as a function of the time delay after the excitation, at lattice temperatures of 20 K and 55 K, respectively [87]. The exciton temperatures rapidly cool toward the lattice temperature within 150 picoseconds. The cooling is slightly faster in GaN than in GaAs [88] and in ZnSe [89]. Since the deformation potential interaction with the acoustic phonons is the dominant mechanism responsible for the cooling of the exciton in this regime, the decrease in exciton temperature can be modelled with a standard deformation potential theory. The energy loss rate due to the deformation potential scattering is [90, 91]

$$\left\langle \frac{\mathrm{d}E}{\mathrm{d}t} \right\rangle = \frac{8\sqrt{2}}{\pi^{3/2}} \frac{(m_x)^{5/2} D^2}{\rho \hbar^4} (k_B T)^{3/2} \left(1 - \frac{T_L}{T}\right) \tag{17}$$

where m_x is the average mass of the exciton, D is the acoustic deformation potential for the exciton, is the mass density and T_L is the lattice temperature. The dashed lines in figure 4 are fitted with the above energy loss rate equation. The deduced value of deformation potential from the fitting is 13 ± 1 eV, close to those obtained by other methods [92].

6. Exciton–phonon interaction in nitride low dimensional structures

Exciton–phonon interactions in low dimensional structures are more complicated due to the effects of quantum confinements on the electronic states and to the modification of phonon modes [21]. In II–VI and GaAs-based quantum wells (QWs) or superlattices, when the temperature dependent excitonic linewidth is studied, a reduction in exciton–LO phonon coupling strength [93–96] with a decrease in QW thickness has been reported. This reduced coupling strength is due to the phonon wave vector q-dependent Fröhlich interaction [21] and to the smaller density of states available to accommodate the scattered exciton [94]. At some certain values of QW thickness, where the separation of the confined states matches the LO phonon energy, an enhancement in the exciton–LO phonon coupling strength is observed [95, 97]. The observation of different values of Huang–Rhys factor in InGaAs/InP QWs was attributed to the difference in localization of the exciton in the plane of QWs [98, 99]. Since the hole has a larger effective mass than the electron, it is localized more easily. This leads to a charge separation between the localized hole and the delocalized electron. The difference in charge separation is responsible for the observation of different values of the exciton–phonon coupling strength.

In the case of quantum dots (QDs), the situation is more complicated, and conflicting results have been reported. Based on the wave vector q-dependent Fröhlich interaction, it was first argued that due to the strong quantum confinement, which enhances the overlap of electron and hole wave functions, the exciton–LO phonon Fröhlich interaction should vanish in small QDs [100]. A reduced coupling strength was observed experimentally in CdSe QDs [101]. By using a donor-like exciton model and an uncorrelated electron–hole wave function, a size-independent coupling strength was predicted and observed experimentally [102]. The charge neutrality makes the exciton–phonon coupling strength decrease in small QDs. However, this decreasing polar coupling is accompanied by an increasing coupling to short wavelength phonons. These two effects may exactly compensate each other and a size-independent

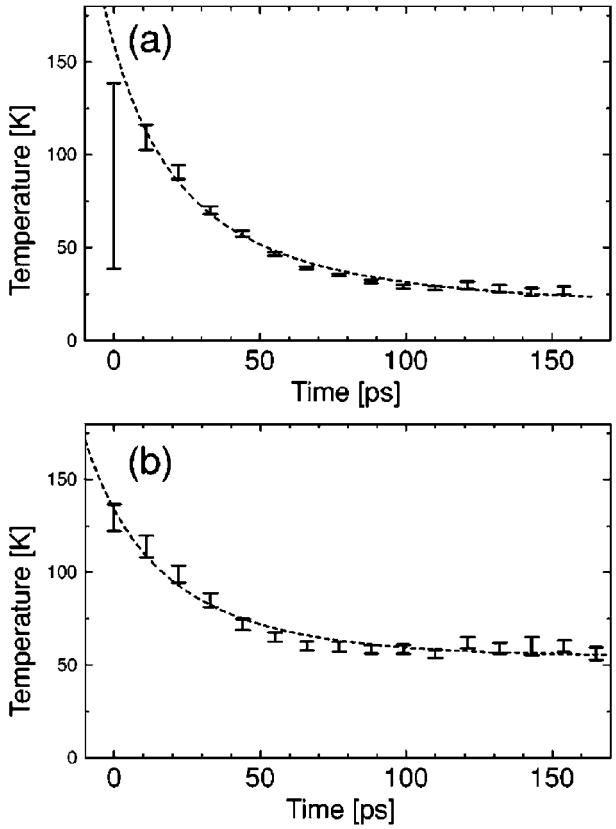

Figure 5. The temperature of the exciton in a GaN sample as a function of the time delayed after the excitation pulse. The temperatures were obtained by fitting the high energy tail of the first LO phonon replica with equation (14.14). The measurements were performed at lattice temperature of 20 K (a) and 55 K (b). The dashed lines are obtained from fits to the data using equation (17) (after [87]).

coupling strength would be expected [102]. In another report, by taking into account the valance band degeneracy and the conduction band nonparabolicity, the LO phonon coupling strength was shown to decrease first, then increase below a certain value of QD size [103]. However, the calculated absolute value of Huang–Rhys factor by this model is significantly smaller than the experimental observations. To explain the experimental observations of much larger Huang–Rhys factor in QDs, a nonadiabatic treatment of the exciton–phonon system has been considered [104, 105]. The calculation showed that the effects of nonadiabaticity are responsible for the observed enhancement of phonon-assisted excitonic transition probabilities. Alternatively, the localization of hole at the surface of QDs [106], and the spatial separation of the electron and the hole distributions of charge density, as a result of particular quantum confinement and piezoelectric potential in the QDs [107], were used to explain the enhanced phonon-assisted processes.

Compared with II–VI and other III–V semiconductors, the exciton–phonon interactions in GaN-based QWs and QDs are less studied. Moreover, the reported results are controversial, both reduced and enhanced exciton–phonon interaction have been reported in nitride low dimensional structures. In the temperature dependent PL study of GaN/AlGaN QDs [108], a

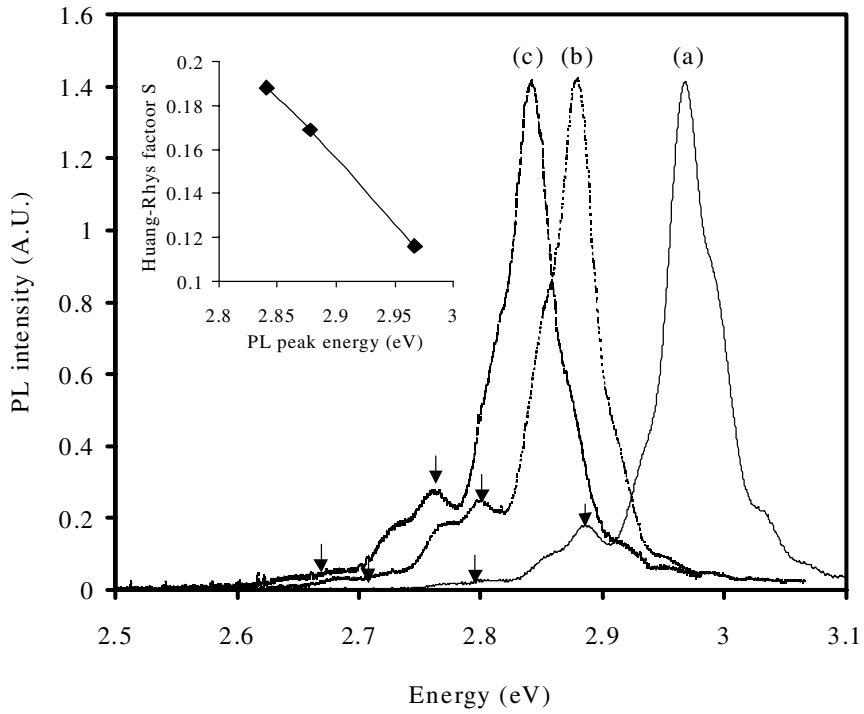

Figure 6. (a), (b) and (c) represent the PL spectra measured at 8 K for three $Ga_{1-x}In_xN$/GaN QD samples. The LO phonon replicas are indicated as arrows in the figure. The inset of the figure shows the *S* factor as a function of zero phonon peak energy.

slow red shift of the PL peak energy (compared with the shift of GaN band gap) was found when the temperature was increased. This slow red shift was explained within the picture of reduced exciton–phonon coupling strength in the QDs. In fact, the slow shift of PL peak energy has several origins. Since the inhomogeneous linewidth of the PL of QDs is very large [108], exciton localization and thermally activated exciton transfer between QDs may occur when the temperature is changed. These processes will lead to a complicated temperature evolution of PL of QDs. Moreover, screening of the built-in electric field, induced by spontaneous and piezoelectric polarization, may be more important at high temperature due to the thermal activation of carriers [109]. To get a reliable strength of exciton–phonon interaction from the temperature dependent PL study, these possibilities have to be considered. In another temperature dependent PL study of GaN/AlGaN superlattices [110], a fast red shift of PL peak energy and a large broadening of PL linewidth (about 30 meV from 150 K to 300 K) were observed when the temperature exceeds 150 K.

Despite the temperature dependent PL studies, LO phonon-assisted excitonic recombinations have been observed in GaN-based low dimensional structures. Strong LO phonon replicas have been observed in low temperature PL spectra of GaInN/GaN QWs [111, 112], GaN/AlGaN QWs [113, 114], and GaInN/GaN QDs [115]. The observed Huang–Rhys factor *S* at low temperature is in a range from 0.07 to 0.8, much larger than those observed in bulk GaN. This indicates that the exciton–phonon interaction is greatly enhanced in these low dimensional structures. The experimental results [111, 114] suggested that the symmetric properties of QWs, together with the alloy disorder, are responsible for the observed large

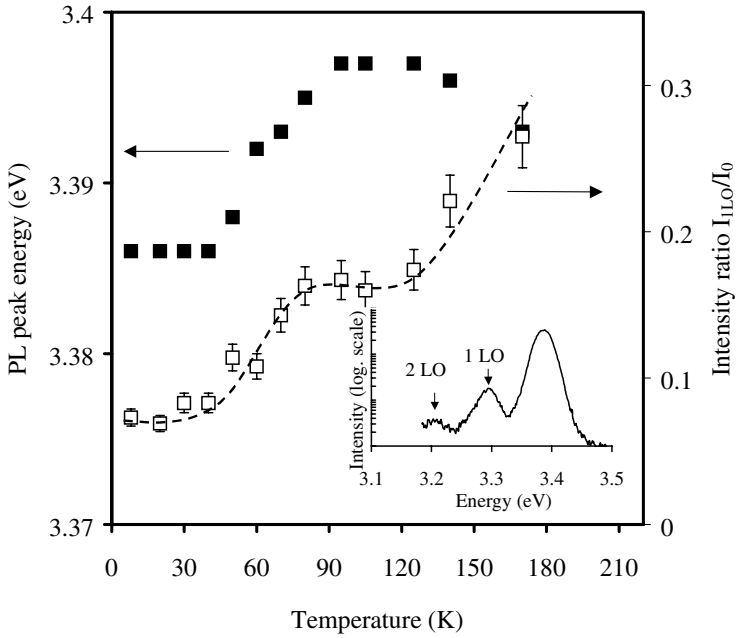

Figure 7. The intensity ratio of the first LO phonon replica relative to that of the zero phonon peak, and the peak energy of the zero phonon peak, measured from a GaN/$Al_{0.17}Ga_{0.83}N$ multiple QW sample, as a function of temperature. The inset of the figure shows a PL spectrum taken at 8 K. Note the logarithmic scale of the PL intensity.

S factor. Further PL studies of GaInN/GaN QWs and QDs show that the value of *S* factor depends strongly on the thickness of QWs or on the height of QDs. A continuous increase in *S* factor with an increase in thickness of QWs or height of QDs has been observed. A typical size dependent PL study of $Ga_{1-x}In_xN$/GaN QD samples is shown in figure 6. The indium composition in all samples is the same and is in a range of 0.15 to 0.2. Microscopic structural characterizations showed that the height of QDs is in a range of 2–5 nm, whereas the full width at half height is from 5 to 10 nm [115]. The PL spectra in the figure are normalized at the same peak intensity. Obviously, an increase in QD size from sample (a) to (c) is manifested by a decrease in PL peak energy. The 1LO and 2LO phonon replicas, as indicated by arrows in the figure, are clearly seen in each spectrum. The energy separation is 91 meV, which is very close to the energy of the LO phonon in bulk wurtzite GaN. By fitting the spectrum with Gaussian functions, the Huang–Rhys factor *S* is obtained. The *S* factor is plotted versus the zero phonon peak energy in the inset of the figure. An increase in *S* factor with a decrease in PL energy shows that the exciton–phonon interaction is stronger in larger QDs.

Since the Huang–Rhys factor depends strongly on the distributions of the density of electron and hole charges, we speculate that the charge distribution has been changed in these QDs. A characteristic feature in GaInN/GaN low dimensional structures is the strong internal electric field caused by piezoelectric and spontaneous polarizations. Such an electric field can be as large as 2.45 MV cm^{-1}. A direct effect of such an electric field on the photo-generated electron–hole pairs is the progressive separation of electron and hole charge density with an increase in QD height. The reduced overlap of electron and hole charge density is responsible for the larger *S* factor observed in larger QDs. By using the same Hamiltonian of exciton–LO phonon interaction in bulk GaN, and by using the electron and hole wave functions described

in [116], the calculated values of S factor fairly well agree with the experimental observation [117]. The calculation predicts that the in-plane localization of excitons in QWs also enhances the phonon-assisted recombinations.

It is known that temperature has a great influence on the phonon-assisted recombination processes. Within the theory of Segall and Mahan [27], where the phonon-assisted excitonic transition probability depends on the kinetic energy of the exciton, a continuous increase in intensity ratio I_{nLO}/I_0 with an increase in temperature would be expected. This increase has been observed in bulk GaN as shown in the inset of figure 1. The temperature dependent LO phonon-assisted recombinations in GaN-based low dimensional structures was studied recently. Figure 7 shows the intensity ratio of the first LO phonon replica to that of the zero phonon peak, as well as the PL peak energy of the zero phonon peak, measured from a $GaN/Al_{0.17}Ga_{0.83}N$ multiple QW sample, as a function of the temperature. The well width is 16 monolayers (ML) i.e., 4.14 nm, and the barrier width is 30 nm. The expected electric field in the QWs is about 814 kV cm^{-1} [118]. An example of a PL spectrum taken at 8 K is shown in the inset of the figure. Note the logarithmic scale of the PL intensity. Two replicas and a main zero phonon peak are clearly seen. The separation between adjacent peaks is about 92 meV, which is in excellent agreement with the LO phonon energy in GaN. With an increase in temperature, the PL peak energy approximately tracks the band gap of bulk GaN until 50 K, above which a blue shift is observed. This blue shift is known as thermal delocalization of excitons from the '2 ML' to '1 ML' region, where '2 ML' ('1 ML') represent places in QWs where the well thickness is 2 ML (1 ML) thicker than the average thickness [118]. It is interesting to note that the intensity ratio of I_{1LO}/I_0 is nearly constant in the region (i.e., from 80 K to 125 K) where the blue shift of PL peak energy is observed, while, in other temperature ranges, it increases with the temperature. The increase in the intensity ratio I_{1LO}/I_0 with the temperature can be understood, similarly to the case of bulk GaN, as a result of the thermal enhancement of the phonon-assisted excitonic transition probability. The small variation of the ratio in the temperature range of 80 K to 125 K can be understood as a result of the change in Huang–Rhys factor S. As discussed above, the S factor depends on the thickness of the QW. The S factor, and thus the intensity ratio I_{1LO}/I_0, is larger in the '2 ML' region than in the '1 ML' region. The constant value of I_{1LO}/I_0 in the temperature range of 80 K to 125 K is a result of a balance between two competitive processes: (1) a thermally enhanced phonon-assisted transition probability and (2) a thermally activated transfer of excitons from the '2 ML' to '1 ML' region, which leads to a reduction of S factor and concomitantly a reduction in I_{1LO}/I_0.

Acknowledgments

The authors are grateful to B Gil for valuable advice and a sanity check of the manuscript. We are particularly grateful to Professor P Y Yu for illuminating discussions about exciton–phonon interactions and valuable advice, to Dr M Leroux for reviewing the first draft manuscript and providing the electronic data of figure 1, and to Dr S K Hark for reading the first draft manuscript and valuable suggestions. Results presented in figures 6 and 7 were taken from samples prepared for us by Nicolas Grandjean. X B Zhang acknowledges the hospitality of the University of Montpellier II and the French Ministry of Education for financial support. This work was partly supported by the EEC under contract HPRN-CF1949-00132 CERMONT.

References

[1] Nakamura S 1999 *Semicond. Sci. Technol.* **14** R27

[2] Lambrecht W R L and Segall B 1998 *Semiconductors and Semimetals* vol 50, ed J I Pankove and T D Moustakas (San Diego: Academic) pp 369–402
[3] Suzuki M and Uenoyama T 1998 *Group III Nitride Semiconductor Compound, Physics and Applications* ed B Gil (Oxford: Clarendon) pp 307–42
[4] Gil B 1999 *Semiconductors and Semimetals* vol 57, ed J I Pankove and T D Moustakas (San Diego: Academic) pp 209–74
[5] Karch K, Wagner J-M and Bechstedt F 1998 *Phys. Rev.* B **57** 7043
[6] Miwa K and Fukumoto A 1993 *Phys. Rev.* B **48** 7897
[7] Wagner J-M and Bechstedt F 2000 *Phys. Rev.* B **62** 4526
[8] Kim K, Walter R, Lambrecht L and Segall B 1994 *Phys. Rev.* B **50** 1502
[9] Siegle H, Kaczmarczyk G, Filippidis L, Litvinchuk A P, Hoffmann A and Thomsen C 1997 *Phys. Rev.* B **55** 7000
[10] Coffey D and Bock N 1999 *Phys. Rev.* B **59** 5799
[11] Davydov V Yu *et al* 1999 *Phys. Status Solidi* b **216** 779
[12] Davydov V Yu, Kitaev Yu E, Goncharuk I N, Smirnov A N, Graul J, Semchinova O, Uffmann D, Smirnov M B, Mirgorodsky A P and Evarestov R A 1998 *Phys. Rev.* B **58** 12 899
[13] Kaczmarczyk G *et al* 2000 *Appl. Phys. Lett.* **76** 2122
[14] Azuhata T, Sota T, Suzuki K and Nakamura S 1995 *J. Phys.: Condens. Matter* **7** L129
[15] Filippidis L, Siegle H, Hoffman A, Thomsen C, Karch K and Bechstedt F 1996 *Phys. Status Solidi* b **198** 621
[16] Demangeot F, Frandon J, Renucci M A, Briot O, Gil B and Aulombard R L 1996 *Solid State Commun.* **100** 207
[17] Klochikhin A A, Davydov V Yu, Goncharuk I N, Smirnov A N, Nikolaev A E, Baidakova M V, Aderhold J, Graul J, Stemmer J and Semchinova O 2000 *Phys. Rev.* B **62** 2522
[18] Bungaro C and de Gironcoli S 2000 *Appl. Phys. Lett.* **76** 2101
[19] Bechstedt F and Grille H 1999 *Phys. Status Solidi* b **216** 761
[20] Yu SeGi, Kim K W, Bergman L, Dutta M, Stroscio M A and Zavada J M 1998 *Phys. Rev.* B **58** 15 283
[21] Yu P Y and Cardona M 1996 *Fundamentals of Semiconductors, Physics and Materials Properties* (Berlin: Springer)
[22] Rudin S, Reinecke T L and Segall B 1990 *Phys. Rev.* B **42** 11 218
[23] Weisbuch C and Ulbrich R G 1982 *Light Scattering in Solids III* ed M Cardona and G Güntherodt (Berlin: Springer) p 210
[24] Cohen E and Sturge M D 1982 *Phys. Rev.* B **25** 3828
[25] Yu P Y 1979 *Excitons* ed K Cho (Berlin: Springer) p 211
[26] Lee B C, Kim K W, Dutta M and Stroscio M A 1997 *Phys. Rev.* B **56** 997
[27] Segall B and Mahan G D 1968 *Phys. Rev.* **171** 935
[28] Gross E, Permogorov S and Razbirin B 1966 *J. Phys. Chem. Solids* **27** 1647
[29] Klyuchikhin A A, Permogorov S A and Reznitski A N 1976 *Sov. Phys.–JETP* **44** 1176
[30] Weiher R L and Tait W C 1968 *Phys. Rev.* **166** 791
[31] Permogorov S 1982 *Excitons* ed E I Rashba and M D Sturge (Amsterdam: North-Holland) p 179
[32] O'Connel-Bronin A A and Plekhanov V G (1979) *Phys. Status Solidi* b **95** 75
[33] Huang K and Rhys A 1950 *Proc. R. Soc.* A **204** 406
[34] Gurskii A L and Viotikov S V 1999 *Solid State Commun.* **112** 339
[35] Duke C B and Mahan G D 1965 *Phys. Rev.* **139** A1965
[36] Soltani M, Certier M, Evrard R and Kartheuser E 1995 *J. Appl. Phys.* **78** 5626
[37] Hopfield J J 1959 *J. Phys. Chem. Solids* **10** 110
[38] Dingle R, Sell D D, Stokowski S E and Ilegems M 1971 *Phys. Rev.* B **4** 1211
[39] Leroux M and Gil B 1999 *Properties, Processing and Applications of Gallium Nitride and Related Semiconductors* ed J Edgar *et al* (London: Inspec, IEE) p 58
[40] Leroux M, Grandjean N, Beaumont B, Nataf G, Semond F, Massies J and Gibart P 1999 *J. Appl. Phys.* **86** 3721
[41] Korona K P, Wysmolek A, Baranowski J M, Pakula K, Bergman J P, Monemar B, Grzegory I and Porowski S 1998 *Mater. Res. Soc.* **482** 501
[42] Le Vaillant Y-M 1999 *Ph.D Thesis* Universite de Montpellier II, p 130
[43] Oh E, Lee S K, Park S S, Lee K Y, Song I J and Han J Y 2001 *Appl. Phys. Lett.* **78** 273
[44] Gurskii A L, Voitikov S V, Hamadeh H, Kalisch H, Heuken M and Heime K 2000 *J. Cryst. Growth* **214/215** 567
[45] Wojdak M, Wysmolek A, Pakula K and Baranowski J M 1999 *Phys. Status Solidi* b **216** 95
[46] Kovalev D, Averboukh B, Volm D, Meyer B K, Amano H and Akasaki I 1996 *Phys. Rev.* B **54** 2518

[47] Liu W, Li M F, Xu S J, Uchida K and Matsumoto K 1998 *Semicond. Sci. Technol.* **13** 769
[48] Xu S J, Liu W and Li M F 2000 *Appl. Phys. Lett.* **77** 3376
[49] Buyanova I A, Bergman J P, Monemar B, Amano H and Akasaki I 1997 *Mater. Sci. Eng.* B **50** 130
[50] An H Y, Cha O H, Kim J H, Yang G M, Lim K Y, Suh E-K and Lee H J 1999 *J. Appl. Phys.* **85** 2888
[51] Sumiya M, Ohnishi T, Tanaka M, Ohtomo A, Kawasaki M, Yoshimoto M, Koinuma H, Ohtsuka K and Fuke S 1999 *Mater. Res. Soc.* **537** G 6.23
[52] Sherriff R E, Reynolds D C, Look D C, Jogai B, Hoelscher J E, Collins T C, Cantwell G and Harsch W C 2000 *J. Appl. Phys.* **88** 3454
[53] Litvinenko K, Birkedal D, Lyssenko V G and Hvam J M 1999 *Phys. Rev.* B **59** 10 255
[54] Logothetidis S, Cardona M, Lautenschlager P and Garriga M 1986 *Phys. Rev.* B **34** 2458
[55] Lee J, Koteles E S and Vassell M O 1986 *Phys. Rev.* B **33** 5512
[56] Benzaquen R, Leonelli R and Charbonneau S 1999 *Phys. Rev.* B **59** 1973
[57] Fischer A J, Shan W, Song J J, Chang Y C, Horning R and Goldenberg B 1997 *Appl. Phys. Lett.* **71** 1981
[58] Viswanath A K, Lee J I, Kim D, Lee C R and Leem J Y 1998 *Phys. Rev.* B **58** 16 333
[59] Chichibu S, Okumura H, Nakamura S, Feuillet G, Azuiiata T, Sota T and Yoshida S 1997 *Japan. J. Appl. Phys.* **36** 1976
[60] Korona K P, Wysmolek A, Pakula K, Stepniewski R, Baranowski J M, Grzegory I, Lucznik B, Wroblewski M and Porowski S 1996 *Appl. Phys. Lett.* **69** 788
[61] Siozade L, Colard S, Mihailovic M, Leymarie J, Vasson A, Grandjean N, Leroux M and Massies J 1999 *Phys. Status Solidi* b **216** 73
[62] Li C F, Huang Y S, Malikova L and Pollak F H 1997 *Phys. Rev.* B **55** 9251
[63] Petalas J, Logothetidis S, Boultadakis S, Alouani M and Wills J M 1995 *Phys. Rev.* B **52** 8082
[64] Fischer A J, Shan W, Park G H, Song J J, Kim D S, Yee D S, Horning R and Goldenberg B 1997 *Phys. Rev.* B **56** 1077
[65] Tchounkeu M, Briot O, Gil B, Alexis J P and Aulombard R-L 1996 *J. Appl. Phys.* **80** 5352
[66] Lee D, Johnson A M, Zucker J E, Feldman R D and Austin R F 1991 *J. Appl. Phys.* **69** 6722
[67] Fischer A J *et al* 1994 *Phys. Rev. Lett.* **73** 2368
[68] Makino T, Chia C H, Tuan N T, Segawa Y, Kawasaki M, Ohtomo A, Tamura Y and Koinuma H 2000 *Appl. Phys. Lett.* **76** 3549
[69] Young J F, Gong T, Fauchet P M and Kelly P J 1994 *Phys. Rev.* B **50** 2208
[70] Shah J 1978 *Solid State Electron.* **21** 43
[71] Shah J 1998 *Hot Electrons in Semiconductors Physics and Devices* ed N Balkan (Oxford: Clarendon) p 55
[72] Binet F and Duboz J Y 1999 *Phys. Rev.* B **60** 4715
[73] Shan W *et al* 1998 *J. Appl. Phys.* **83** 455
[74] Zukauskas A Z, Tamulaitis G, Gaska R, Shur M S, Khan M A and Yang J W 1999 *Phys. Status Solidi* b **216** 495
[75] Yu P Y 2001 private communication
[76] Sheih S J, Tsen K T, Ferry D K, Botchkarev A, Sverdlov B, Salvador A and Morkoc H 1995 *Appl. Phys. Lett.* **67** 1757
[77] Tsen K T, Ferry D K, Botchkarev A, Sverdlov B, Salvador A and Morkoc H 1998 *Appl. Phys. Lett.* **72** 2132
[78] Tsen K T, Joshi R P, Ferry D K, Botchkarev A, Sverdlov B, Salvador A and Morkoc H 1996 *Appl. Phys. Lett.* **68** 2990
[79] Kuball M, Hayes J M, Shi Y and Edgar J H 2000 *Appl. Phys. Lett.* **77** 1958
[80] Bergman L, Alexson D, Murphy P L, Nemanich R J, Dutta M, Stroscio M A, Balkas C, Shin H and Davis R F 1999 *Phys. Rev.* B **59** 12 977
[81] Klemens P G 1966 *Phys. Rev.* **148** 845
[82] Ridley B K 1996 *J. Phys.: Condens. Matter* **8** L511
[83] Ye H, Wicks G W and Fauchet P M 1999 *Appl. Phys. Lett.* **74** 711
[84] Ye H, Wicks G W and Fauchet P M 2000 *Appl. Phys. Lett.* **77** 1185
[85] Tsen K T, Ferry D K, Botchkarev A, Sverdlov B, Salvador A and Morkoc H 1997 *Appl. Phys. Lett.* **71** 1852
[86] Tamulaitis G, Zukauskas A Z, Yang J W, Khan M A, Shur M S and Gaska R 1999 *Appl. Phys. Lett.* **75** 2277
[87] Hagele D, Zimmermann R, Oestreich M, Hofmann M R, Ruhle W W, Meyer B K, Amano H and Akasaki I 1999 *Phys. Rev.* B **59** R7797
[88] Leo K, Ruhle W W and Ploog K 1988 *Phys. Rev.* B **38** 1947
[89] Poweleit C D, Smith L M and Jonker B T 1997 *Phys. Rev.* B **55** 5062
[90] Ulbrich R 1973 *Phys. Rev.* B **8** 5719
[91] Snoke D W and Wolfe J P 1990 *Phys. Rev.* B **42** 7876
[92] Morkoc H 1999 *Nitride Semiconductors and Devices* (Berlin: Springer) p 245

[93] Pollak F H 1993 *Phonons in Semiconductor Nanostructures (NATO Advanced Study Institute, Series E: Applied Sciences vol 236)* ed J P Leburton, J Pascual and C Sotomayor Torres (New York: Plenum) p 341
[94] Pelekanos N T, Ding J, Hagerott M, Nurmikko A V, Luo H, Samarth N and Furdyna J K 1992 *Phys. Rev.* B **45** 6037
[95] Young P M, Runge E, Ziegler M and Ehrenreich H 1994 *Phys. Rev.* B **49** 7424
[96] Nashiki H, Suemune I, Kumano H, Suzuki H, Obinata T, Vesugi K and Nakahara J 1997 *Appl. Phys. Lett.* **70** 2350
[97] Venu Gopal A, Kumar R, Vengurlekar A S, Melin T, Laruelle F and Etienne B 1999 *Appl. Phys. Lett.* **74** 2474
[98] Skolnick M S, Nash K J, Tapster P R, Mowbray D J, Bass S J and Pitt A D 1987 *Phys. Rev.* B **35** 5925
[99] Nash K J, Skolnick M S, Claxton P A and Roberts J S (1989) *Phys. Rev.* B **39** 5558
[100] Schmitt-Rink S, Miller D A B and Chemla D S 1987 *Phys. Rev.* B **35** 8113
[101] Shiang J J, Risbud S H and Alivisatos A P 1993 *J. Chem. Phys.* **98** 8432
[102] Klein M C, Hache F, Ricard D and Flytzanis C 1990 *Phys. Rev.* B **42** 11 123
[103] Nomura S and Kobayashi T 1992 *Phys. Rev.* B **45** 1305
[104] Fomin V M, Gladilin V N, Devreese J T, Pokatilov E P, Balaban S N and Klimin S N 1998 *Phys. Rev.* B **57** 2415
[105] Fomin V M, Gladilin V N, Klimin S N, Devreese J T, Koenraad P M and Wolter J H 2000 *Phys. Rev.* B **61** R2436
[106] Nirmal M, Murray C B and Bawendi M G 1994 *Phys. Rev.* B **50** 2293
[107] Heitz R, Mukhametzhanov I, Stier O, Madhukar A and Bimberg D 1999 *Phys. Rev. Lett.* **83** 4654
[108] Ramvall P, Tanaka S, Nomura S, Riblet P and Aoyagi Y 1999 *Appl. Phys. Lett.* **75** 1935
[109] Riblet P, Hirayama H, Kinodhita A, Hirata A, Sugano T and Aoyagi Y 1999 *Appl. Phys. Lett.* **75** 2241
[110] Bergman L, Dutta M, Stroscio M A, Komirenko S M, Nemanich R J, Eiting C J, Lambert D J H, Kwon H K and Dupuis R D 2000 *Appl. Phys. Lett.* **76** 1969
[111] Smith M, Lin J Y, Jiang H X, Khan A, Chen Q, Salvador A, Botchkarev A, Kim W and Morkoc H 1997 *Appl. Phys. Lett.* **70** 2882
[112] Davidson J A, Dawson P, Wang T, Sugahara T, Orton J W and Sakai S 2000 *Semicond. Sci. Technol.* **15** 497
[113] Alderighi D, Vinattieri A, Bogani F, Colocci M, Gottardo S, Grandjean N and Massies J 2001 *Phys. Status Solidi* a **183** 129
[114] Smith M, Lin J Y, Jiang H X, Salvador A, Botchkarev A, Kim W and Morkoc H 1996 *Appl. Phys. Lett.* **69** 2453
[115] Morel A, Gallart M, Taliercio T, Lefebvre P, Gil B, Allegre J, Mathieu H, Damilano B, Grandjean N and Massies J 2000 *Phys. Status Solidi* a **180** 375
[116] Gallart M, Morel A, Taliercio T, Lefebvre P, Gil B, Allegre J, Mathieu H, Grandjean N, Leroux M and Massies J 2000 *Phys. Status Solidi* a **180** 127
[117] Kalliakos S, Zhang X B, Taliercio T, Lefebvre P, Gil B, Grandjean N, Damilano B and Massies J 2001 unpublished
[118] Gallart M, Lefebvre P, Morel A, Taliercio T, Gil B, Allegre J, Mathieu H, Damilano B, Grandjean N and Massies J 2001 *Phys. Status Solidi* a **183** 61